Research Article Vol. 4, No. 10 / October 2017 / Optica 1214

Entanglement swapping over 100 km optical fiber with independent entangled photon-pair sources

Qi-Chao Sun,[1,2,3,†] Yang-Fan Jiang,[1,2,†] Ya-Li Mao,[1,2,†] Li-Xing You,[4] Wei Zhang,[5] Wei-Jun Zhang,[5] Xiao Jiang,[1,2] Teng-Yun Chen,[1,2] Hao Li,[4] Yi-Dong Huang,[5] Xian-Feng Chen,[3] Zhen Wang,[4] Jingyun Fan,[1,2] Qiang Zhang,[1,2,6] and Jian-Wei Pan[1,2,7]

[1]National Laboratory for Physical Sciences at Microscale and Department of Modern Physics, Shanghai Branch, University of Science and Technology of China, Hefei, Anhui 230026, China
[2]CAS Center for Excellence and Synergetic Innovation Center in Quantum Information and Quantum Physics, Shanghai Branch, University of Science and Technology of China, Hefei, Anhui 230026, China
[3]School of Physics and Astronomy, Shanghai Jiao Tong University, Shanghai 200240, China
[4]State Key Laboratory of Functional Materials for Informatics, Shanghai Institute of Microsystem and Information Technology, Chinese Academy of Sciences, Shanghai 200050, China
[5]Tsinghua National Laboratory for Information Science and Technology, Department of Electronic Engineering, Tsinghua University, Beijing 100084, China
[6]e-mail: qiangzh@ustc.edu.cn
[7]e-mail: pan@ustc.edu.cn

Received 3 July 2017; revised 16 August 2017; accepted 3 September 2017 (Doc. ID 301611); published 4 October 2017

Realizing long-distance entanglement swapping with independent sources in the real-world condition is important for both future quantum networks and fundamental study of quantum theory. Currently, entanglement swapping over a few tens of kilometers of underground optical fiber has been achieved. However, future applications demand entanglement swapping over longer distances in more complicated environments. We exploit two independent 1-GHz-clock sequential time-bin entangled photon-pair sources; develop several automatic stability controls; and successfully implement a field test of entanglement swapping over an optical fiber link of more than 100 km, including coiled, underground, and suspended optical fibers. Our result verifies the feasibility of such technologies for long-distance quantum networks and for many interesting quantum information experiments.

OCIS codes: (060.5565) Quantum communications; (270.5585) Quantum information and processing.

https://doi.org/10.1364/OPTICA.4.001214

1. INTRODUCTION

Entanglement swapping [1,2] is a unique feature of quantum physics. By entangling two independent parties, which have never interacted before, entanglement swapping has been used in studies of physics foundations such as nonlocality [1,3] and wave–particle duality [4]. It is also a central element in quantum networks [5,6], appearing in the form of quantum relay [7–9] and quantum repeater [10,11]. The integrity of an experimental realization of entanglement swapping is ensured only by satisfying the following criteria: proper causal disconnection between relevant events [12,13], and independent quantum sources without a common past [3].

Driven by the application of future quantum networks, there has been significant progress in experimental entanglement swapping since its first experimental demonstration [2]. Quantum interference with independent sources was addressed in a number of experimental settings [14–18]. A quantum relay was simulated with coiled optical fibers in a laboratory environment [19]. Recently, entanglement swapping and quantum teleportation were realized in both free-space and optical fiber links over a distance of about 100 km [20–23], in which the quantum sources shared a common past, the Bell state measurements (BSMs) were performed locally, and the swapped (teleported) photonic qubits were sent over a long distance afterwards for analysis. More recently, several teams succeeded in entanglement swapping and teleportation with high integrity over a fiber network (a few tens of kilometers) in the real world, in which they overcame the challenge in removing the distinguishability between photons from separate quantum sources by defeating the noise in the real world [13,24–26]. To date, there is no report on entanglement swapping with independent sources over optical fiber of 100 km nor with suspended optical fiber, which is more susceptible to the environment but unavoidable for applications in optical fiber networks.

Here, we present an implementation of entanglement swapping in an intercity quantum network, which is composed of about 77 km of optical fiber inside the lab, 25 km of optical fiber outside the lab but kept underground, and 1 km of optical fiber suspended in air outside the lab to account for various types of noise mechanisms in the real world.

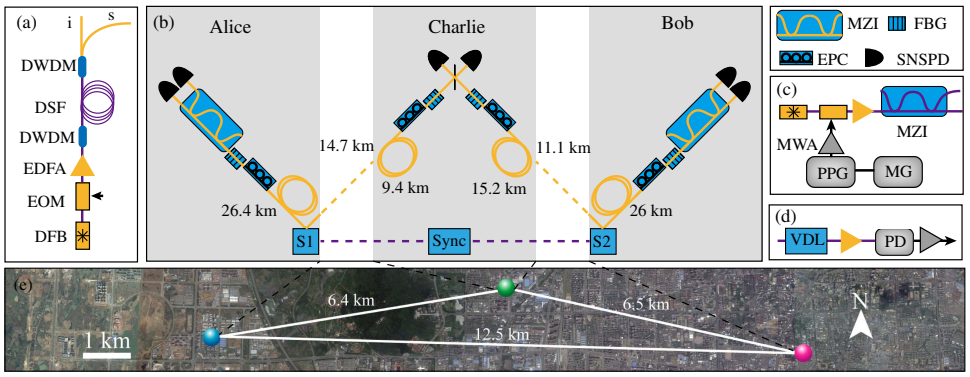

Fig. 1. Scheme of the entanglement swapping experiment. (a) Setup of sequential time-bin entangled photon-pair source. DFB, distributed feedback laser; EOM, electro-optic modulator; EDFA, erbium-doped fiber amplifier; DWDM, dense wavelength-division multiplexing filter; DSF, dispersion-shifted fiber. (b) Experimental realization. Two sequential time-bin entangled photon-pair sources, S1 and S2, are placed in nodes Alice and Bob, respectively. Each of them keeps the idler photons in coiled fibers and distributes the signal photons to Charlie through a deployed optical fiber. The yellow dashed lines represent the deployed fibers and the circles represent the coiled fibers. The total transmission loss of the 77 km coiled optical fiber is about 16 dB, whereas those of the optical fiber deployed in the Alice–Charlie and Bob–Charlie links are 6 dB and 7 dB, respectively. To synchronize the two sources, Charlie prepares 1 GHz laser pulses (Sync) and sends them to Alice and Bob through the deployed optical fiber (represented by the purple dashed lines) to generate the driven signal for their EOMs. Setup: MZI, unbalanced Mach–Zehnder interferometer; EPC, electronic-controlled polarization controller; FBG, fiber Bragg grating; SNSPD, superconducting nanowire single-photon detector. (c) Setup of synchronization signal generation. Charlie first generates laser pulses with a repetition rate of 500 MHz and then doubles them using an MZI with a path difference of 1 ns. MG, microwave generator; PPG, pulse pattern generator; MWA, microwave amplifier. (d) Setup to generate the driven signal for the EOM in (a). VDL, variable-delay line; PD, photodiode. (e) Satellite image of the experimental nodes.

2. EXPERIMENTAL IMPLEMENTATION

A schematic of the sequential time-bin entangled photon-pair source [27–29] is depicted in Fig. 1(a). We carve the continuous-wave (CW) output of a distributed feedback laser (with coherence time of $\tau_c = 300$ μs) periodically into pulses at a rate of 1 GHz with an electro-optical modulator (EOM). The sequential laser pulses differ by $\tau = 1$ ns and a phase difference of $\theta = 2\pi\nu\tau$. After amplification with an erbium-doped fiber amplifier and spectral filtering with dense wavelength-division multiplexing filters (DWDMs), the laser pulses (with a spectrum bandwidth of about 8 GHz and pulse duration of about 60 ps) are fed into a 300 m dispersion-shifted fiber immersed in liquid nitrogen to produce photon pairs via spontaneous four-wave mixing [30–32]. The quantum state of a photon pair produced is given by $|\Theta\rangle = \frac{1}{\sqrt{n}}\sum_{k=0}^{n-1} e^{2ik\theta}|t_k\rangle_s|t_k\rangle_i$, where $t_k = k\tau$ represents time bin k, and i and s are for idler (1555.73 nm) and signal (1549.36 nm) photons, respectively. We single out the signal/idler photons with cascaded DWDM filters with pump photons suppressed by 115 dB.

A schematic of the entanglement swapping experiment is shown in Fig. 1(b), with(out) the gray shaded areas indicating the indoor (outdoor) environment. The two quantum sources are placed 12.5 km apart at nodes Alice and Bob, and BSM is performed at the third node (Charlie) between them, as shown in Fig. 1(e). Alice and Bob hold idler photons with coiled fibers of 26 km while sending signal photons to Charlie. We specifically keep an optical fiber cable of 1 km between Bob and Charlie suspended in air and exposed to sunlight and wind to face inclement weather conditions. The rest deployed fibers are kept underground. The total length of the optical fiber is 103 km with a total transmission loss of ∼29 dB. Upon detection, both idler and signal photons are passed through 4 GHz fiber Bragg gratings (the central wavelength is determined by the device temperature, which is maintained with a stability of 0.01°C), which is about half of the bandwidth of the pump pulses and is therefore sufficient to eliminate the frequency correlation between the twin photons [24]. To synchronize the operation of each node in the quantum network, Charlie keeps a master clock, which sends 75 ps laser pulses to Alice and Bob at 1 GHz, which is used to drive the EOM to synchronize independent quantum sources [see Figs. 1(c) and 1(d), respectively].

In the BSM, it is critical that the signal photons sent by Alice and Bob arrive at a 50:50 beam splitter (BS) simultaneously. However, the arrival time changes drastically due to fluctuation of the effective length of the optical fiber link, which is subjected to the influence of the real world. As shown in Fig. 2, the typical changes in peak-to-peak relative delays between the arrival times of the photons from Alice and Bob are 200 ps, 500 ps, and 1000 ps on rainy days, cloudy days, and sunny days, respectively, which are much larger than the coherent time of the signal photons (∼110 ps). We use the difference between the arrival times of the signal photons from Alice and Bob as error signals and feed them into a delay line to suppress the relative delay to 6 ps under all weather conditions, which is ≪110 ps to ensure high interference visibility. In addition, for each channel, an electronic-controlled polarization controller is used to compensate for the polarization fluctuation caused by the optical fiber.

Before performing entanglement swapping, we characterize the quantum source of Alice (Bob) after entanglement distribution using a Franson-type interferometer. At nodes Alice (Bob) and Charlie, the idler and signal photons are fed into an unbalanced Mach–Zehnder interferometer (MZI) with an arm difference of 1 ns. The interference term in one output of the MZI can be written as $\sum_{k=1}^{n-1} e^{2ik\theta}(1 + e^{i(\theta_s+\theta_i-2\theta)})|t_k\rangle_s|t_k\rangle_i$, where θ_s and θ_i are, respectively, the relative phases induced by MZIs for single and idler photons (see Supplement 1 for details). The outputs of the MZIs are detected by superconducting nanowire

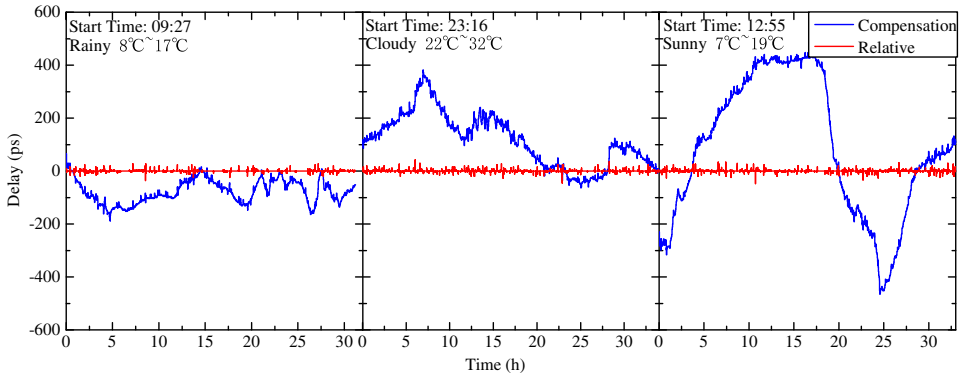

Fig. 2. Typical delay compensation (blue line) and relative delay between the arrival time of photons from Alice and Bob (red line) under different weather conditions. Measured by a TDC with time resolution of 4 ps, the standard deviations of the relative delay in (a), (b), and (c) are 6.7 ps, 6.0 ps, and 6.5 ps, respectively.

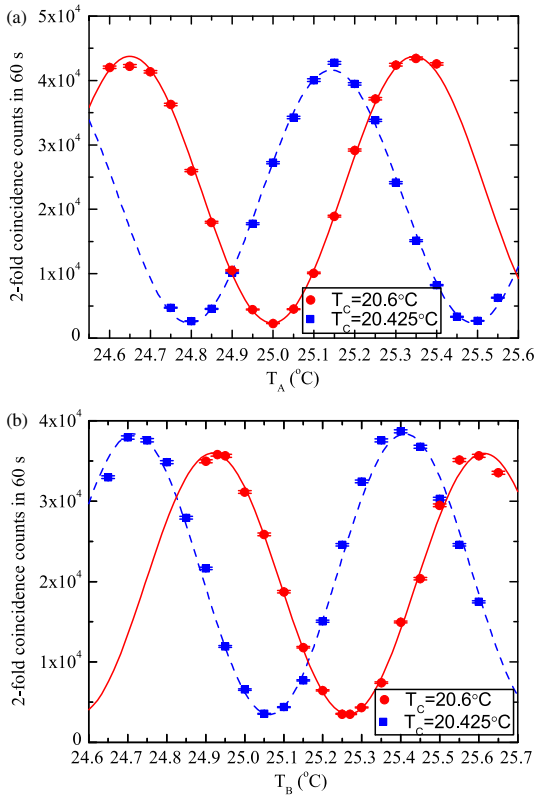

Fig. 3. Two-fold coincidence counts of the sequential time-bin entangled photon pairs distributed by (a) Alice and (b) Bob as functions of the temperature of the MZIs. The measurement results are represented by squares and circles corresponding to Charlie's MZI at temperatures of 20.425°C and 20.6°C, respectively. The error bars indicate one standard deviation calculated from the measured counts assuming Poissonian detection statistics. The visibility of the fitted sinusoidal curves for the squares (circles) is $(89.8 \pm 0.6)\%$ [$(89.5 \pm 1.2)\%$] and $(83.5 \pm 1.5)\%$ [$(82.3 \pm 0.8)\%$] for (a) and (b), respectively.

single-photon detectors (SNSPDs, with 50%–65% detection efficiency, ~100 Hz dark count rate, and ~80 ps time jitter), and the detection results are recorded by time-to-digital converters (TDCs) with 4 ps resolution and analyzed in real-time. The TDCs are synchronized with 10 MHz clocks at Charlie's node.

Figure 3 shows that the measured two-fold coincidence counts between Alice (Bob) and Charlie change sinusoidally as functions of phase (which is dialed by sweeping the temperature of the MZI), with visibility of $(89.8 \pm 0.5)\%$ for Alice's source and $(82.9 \pm 1.2)\%$ for Bob's source. Note that the device temperature is maintained with stability of about 0.005°C and no accidental coincidence counts are subtracted.

3. EXPERIMENTAL RESULTS

In the entanglement swapping experiment, Charlie performs BSM with signal photons sent by Alice and Bob by interfering them on a BS. By detecting them with two SNSPDs and within a delay of 1 ns (for the same time bin or adjacent time bins), the overall state of the two entangled photon pairs, $|\Gamma\rangle_{1,2} = \frac{1}{n}(\sum_{k=0}^{n-1} e^{2ik\theta}|t_k\rangle_{1s}|t_k\rangle_{1i}) \otimes (\sum_{l=0}^{n-1} e^{2il\theta}|t_l\rangle_{2s}|t_l\rangle_{2i})$, can be cast into

$$|\Gamma\rangle_{1,2} \to \frac{1}{n}\left\{\sum_{k=0}^{n-1}\frac{e^{4ik\theta}}{\sqrt{2}n}|t_k\rangle_{1i}|t_k\rangle_{2i}(|\Phi^+\rangle_{s,k}+|\Phi^-\rangle_{s,k}) + \sum_{k=0}^{n-2} e^{i(4k+2)\theta}\left[\frac{1}{\sqrt{2}}(|t_k\rangle_{1i}|t_{k+1}\rangle_{2i}+|t_{k+1}\rangle_{1i}|t_k\rangle_{2i})|\Psi^+\rangle_{s,k} \frac{1}{\sqrt{2}}(|t_k\rangle_{1i}|t_{k+1}\rangle_{2i}-|t_{k+1}\rangle_{1i}|t_k\rangle_{2i})|\Psi^-\rangle_{s,k}\right]\right\},$$

where the four Bell state sets are given by $\{|\Psi^{\pm}\rangle_{s,k} = \frac{1}{\sqrt{2}}(|t_k\rangle_{1s}|t_{k+1}\rangle_{2s} \pm |t_{k+1}\rangle_{1s}|t_k\rangle_{2s})\}$ and $\{|\Phi^{\pm}\rangle_{s,k} = \frac{1}{\sqrt{2}}(|t_k\rangle_{1s}|t_k\rangle_{2s} \pm |t_{k+1}\rangle_{1s}|t_{k+1}\rangle_{2s})\}$.

The Bell states $|\Phi^{\pm}\rangle_{s,k}$ correspond to cases in which the two signal photons are output from the same port of the BS and in the same time bin, which cannot be distinguished using linear optics. The Bell states $|\Psi^{+}\rangle_{s,k}$ and $|\Psi^{-}\rangle_{s,k}$ correspond to cases in which the two signal photons are output in time bins with a delay of 1 ns, although from the same port and from different ports of the BS, respectively. In our experiment, the recovering time of the SNSPD is about 40 ns—much longer than the time delay of two consecutive time bins, so only the Bell states $\{|\Psi_k^-\rangle_{s,k}\}$ are discriminated in the BSM. As a result, their twin photons are projected to an entangled quantum state $|\Psi^-\rangle_{i,k} = \frac{1}{\sqrt{2}}(|t_k\rangle_{1i}|t_{k+1}\rangle_{2i} - |t_{k+1}\rangle_{1i}|t_k\rangle_{2i})$. To verify the entanglement swapping, both Alice and Bob use a MZI with a path difference of 1 ns followed by SNSPDs and implement a conditioned

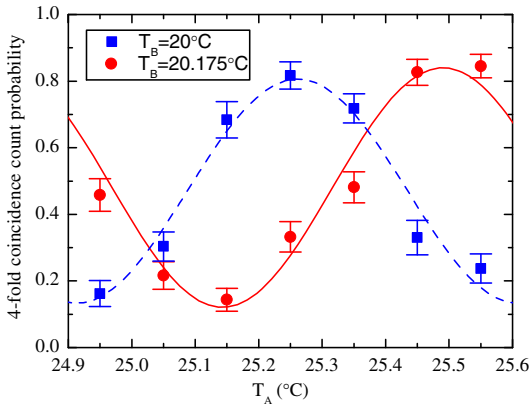

Fig. 4. Four-fold coincidence count probabilities as functions of the temperature of Alice's MZI. The error bars indicate one standard deviation calculated from the measured counts assuming Poissonian detection statistics. Each data point is calculated by using ∼100 four-fold coincidence counts. The visibility of the fitted curve is $(74.8 \pm 8.7)\%$ and $(71.7 \pm 7.2)\%$ for the measured results with $T_B = 20.175$°C and $T_B = 20$°C, respectively.

Franson-type measurement for a time-bin entangled state. The experimental result without subtracting accidental coincidence counts is shown in Fig. 4. The four-fold coincidence counts show a clear interference fringe and the average visibility of the fitted curves is $(73.2 \pm 5.6)\%$. If we assume that the two photons are in a Werner state, we can show that the lower bound of visibility to demonstrate entanglement is 1/3 [33]. The visibility achieved in our experiment clearly exceeds this bound.

4. DISCUSSION

In our experiment, the total transmission loss of the optical fiber link is about 20 dB higher than that in previous field tests with independent sources [26]. By setting the interval between adjacent coherent pump laser pulses equal to that of a conventional time-bin entangled photon-pair source, the event rate of an experiment with a sequential time-bin entangled photon-pair source can be increased three times. The four-fold coincidence count in our experiment is about three counts per hour and each data point is accumulated for more than 30 h. The added coiled fibers also caused a delay drift and polarization fluctuation of the idler photons. We correct the delay drift of the idler photons automatically every 1 s so that the detection results can be recorded in the correct time window. In addition, automatic polarization compensation is used in these channels. Therefore, even the coiled fiber is replaced with the deployed fiber, the system can still work.

The relative low visibility of the entanglement created in entanglement swapping is mainly due to the imperfect sequential time-bin entangled photon-pair sources, which upper bounds the visibility to ∼74% (product of the visibility of two entanglement sources). In our experiment, the average photon-pair number per time bin is $\mu \approx 0.023$ for both sources. The multipair events and the noise photons can decrease the visibility to ∼93.4% and ∼94.4% for Alice's and Bob's sources, respectively (see Supplement 1 for details). The wavelength of the CW laser is controlled with stability of 0.18 pm, resulting in a fluctuation of the relative phase in the entangled state. Assuming the temperature fluctuation follows a Gaussian distribution, it can decrease the visibility to ∼96%. The distortion of the driven signals can also decrease the visibility. The main reason for distortion is the limited bandwidth of the photodiode (PD), which is 45 GHz and 10 GHz for Alice and Bob, respectively. Therefore, by employing a 45 GHz PD in Bob's source, it is possible that the visibility of the swapped entanglement can be increased to ∼80% so that it can be used to demonstrate quantum key distribution [26]. Note that both the event rate and visibility can be improved when entanglement swapping is used in conjunction with quantum memory and entanglement distillation, i.e., a quantum repeater [10,11].

5. CONCLUSION

In summary, we have demonstrated entanglement swapping with two independent sources 12.5 km apart using optical fiber of 103 km. Compared with previous experiments with independent sources, we have increased the length of the optical fiber from metropolitan distance to intercity distance. Specifically, suspended optical fiber is used in our experiment. The transmission loss and stability of the optical fiber channel in our experiment are enough to match those of typical underground deployed optical fiber of more than 100 km [34]. To increase the event rate, we updated the sources to 1 GHz sequential time-bin entangled photon-pair sources. In addition, we improve the polarization and delay compensation system. Our results show that realizing entanglement swapping between two cities is technically feasible, even if more suspended fiber is used (see Supplement 1 for more discussion). Moreover, the configuration in our experiment allows a space-like separation between any two measurements of those performed in the three nodes, and various time-space relations can be achieved by combining both a coiled optical fiber and a deployed optical fiber. This distinguishing feature together with the independent sources makes our setup a promising platform for many interesting fundamental tests.

Funding. National Fundamental Research Program (2013CB336800); National Natural Science Foundation of China (NSFC); Chinese Academy of Sciences (CAS); 10000-Plan of Shandong Province; Quantum Ctek Co., Ltd.

Acknowledgment. The authors thank M.-H. Li, B. Wang, X.-L. Wang, and Y. Liu for enlightening discussions.

†These authors contributed equally to this work.

See Supplement 1 for supporting content.

REFERENCES

1. M. Żukowski, A. Zeilinger, M. Horne, and A. Ekert, ""Event-ready-detectors" Bell experiment via entanglement swapping," Phys. Rev. Lett. **71**, 4287–4290 (1993).
2. J.-W. Pan, D. Bouwmeester, H. Weinfurter, and A. Zeilinger, "Experimental entanglement swapping: entangling photons that never interacted," Phys. Rev. Lett. **80**, 3891–3894 (1998).
3. C. Branciard, N. Gisin, and S. Pironio, "Characterizing the nonlocal correlations created via entanglement swapping," Phys. Rev. Lett. **104**, 170401 (2010).
4. A. Peres, "Delayed choice for entanglement swapping," J. Mod. Opt **47**, 139–143 (2000).

5. J. I. Cirac, P. Zoller, H. J. Kimble, and H. Mabuchi, "Quantum state transfer and entanglement distribution among distant nodes in a quantum network," Phys. Rev. Lett. **78**, 3221–3224 (1997).
6. H. J. Kimble, "The quantum internet," Nature **453**, 1023–1030 (2008).
7. E. Waks, A. Zeevi, and Y. Yamamoto, "Security of quantum key distribution with entangled photons against individual attacks," Phys. Rev. A **65**, 052310 (2002).
8. B. Jacobs, T. Pittman, and J. Franson, "Quantum relays and noise suppression using linear optics," Phys. Rev. A **66**, 052307 (2002).
9. D. Collins, N. Gisin, and H. D. Riedmatten, "Quantum relays for long distance quantum cryptography," arXiv:quant-ph/0311101 (2003).
10. H. J. Briegel, W. Dur, J. I. Cirac, and P. Zoller, "Quantum repeaters: the role of imperfect local operations in quantum communication," Phys. Rev. Lett. **81**, 5932–5935 (1998).
11. L. M. Duan, M. D. Lukin, J. I. Cirac, and P. Zoller, "Long-distance quantum communication with atomic ensembles and linear optics," Nature **414**, 413–418 (2001).
12. X.-S. Ma, S. Zotter, J. Kofler, R. Ursin, T. Jennewein, C. Brukner, and A. Zeilinger, "Experimental delayed-choice entanglement swapping," Nat. Phys. **8**, 479–484 (2012).
13. B. Hensen, H. Bernien, A. E. Dreau, A. Reiserer, N. Kalb, M. S. Blok, J. Ruitenberg, R. F. L. Vermeulen, R. N. Schouten, C. Abellan, W. Amaya, V. Pruneri, M. W. Mitchell, M. Markham, D. J. Twitchen, D. Elkouss, S. Wehner, T. H. Taminiau, and R. Hanson, "Loophole-free Bell inequality violation using electron spins separated by 1.3 kilometres," Nature **526**, 682–686 (2015).
14. T. Yang, Q. Zhang, T. Y. Chen, S. Lu, J. Yin, J. W. Pan, Z. Y. Wei, J. R. Tian, and J. Zhang, "Experimental synchronization of independent entangled photon sources," Phys. Rev. Lett. **96**, 110501 (2006).
15. R. Kaltenbaek, B. Blauensteiner, M. Zukowski, M. Aspelmeyer, and A. Zeilinger, "Experimental interference of independent photons," Phys. Rev. Lett. **96**, 240502 (2006).
16. M. Halder, A. Beveratos, N. Gisin, V. Scarani, C. Simon, and H. Zbinden, "Entangling independent photons by time measurement," Nat. Phys. **3**, 692–695 (2007).
17. R. Kaltenbaek, R. Prevedel, M. Aspelmeyer, and A. Zeilinger, "High-fidelity entanglement swapping with fully independent sources," Phys. Rev. A **79**, 040302 (2009).
18. R. M. Stevenson, J. Nilsson, A. J. Bennett, J. Skiba-Szymanska, I. Farrer, D. A. Ritchie, and A. J. Shields, "Quantum teleportation of laser-generated photons with an entangled-light-emitting diode," Nat. Commun. **4**, 2859 (2013).
19. H. de Riedmatten, I. Marcikic, W. Tittel, H. Zbinden, D. Collins, and N. Gisin, "Long distance quantum teleportation in a quantum relay configuration," Phys. Rev. Lett. **92**, 047904 (2004).
20. J. Yin, J.-G. Ren, H. Lu, Y. Cao, H.-L. Yong, Y.-P. Wu, C. Liu, S.-K. Liao, F. Zhou, Y. Jiang, X.-D. Cai, P. Xu, G.-S. Pan, J.-J. Jia, Y.-M. Huang, H. Yin, J.-Y. Wang, Y.-A. Chen, C.-Z. Peng, and J.-W. Pan, "Quantum teleportation and entanglement distribution over 100-kilometre free-space channels," Nature **488**, 185–188 (2012).
21. X.-S. Ma, T. Herbst, T. Scheidl, D. Wang, S. Kropatschek, W. Naylor, B. Wittmann, A. Mech, J. Kofler, E. Anisimova, V. Makarov, T. Jennewein, R. Ursin, and A. Zeilinger, "Quantum teleportation over 143 kilometres using active feed-forward," Nature **489**, 269–273 (2012).
22. T. Herbst, T. Scheidl, M. Fink, J. Handsteiner, B. Wittmann, R. Ursin, and A. Zeilinger, "Teleportation of entanglement over 143 km," Proc. Natl. Acad. Sci. USA **112**, 14202–14205 (2015).
23. H. Takesue, S. D. Dyer, M. J. Stevens, V. Verma, R. P. Mirin, and S. W. Nam, "Quantum teleportation over 100 km of fiber using highly efficient superconducting nanowire single-photon detectors," Optica **2**, 832–835 (2015).
24. Q.-C. Sun, Y.-L. Mao, S.-J. Chen, W. Zhang, Y.-F. Jiang, Y.-B. Zhang, W.-J. Zhang, S. Miki, T. Yamashita, H. Terai, X. Jiang, T.-Y. Chen, L.-X. You, X.-F. Chen, Z. Wang, J.-Y. Fan, Q. Zhang, and J.-W. Pan, "Quantum teleportation with independent sources and prior entanglement distribution over a network," Nat. Photonics **10**, 671–675 (2016).
25. R. Valivarthi, M. I. G. Puigibert, Q. Zhou, G. H. Aguilar, V. B. Verma, F. Marsili, M. D. Shaw, S. W. Nam, D. Oblak, and W. Tittel, "Quantum teleportation across a metropolitan fibre network," Nat. Photonics **10**, 676–680 (2016).
26. Q.-C. Sun, Y.-L. Mao, Y.-F. Jiang, Q. Zhao, S.-J. Chen, W. Zhang, W.-J. Zhang, X. Jiang, T.-Y. Chen, L.-X. You, L. Li, Y.-D. Huang, X.-F. Chen, Z. Wang, X. Ma, Q. Zhang, and J.-W. Pan, "Entanglement swapping with independent sources over an optical-fiber network," Phys. Rev. A **95**, 032306 (2017).
27. H. De Riedmatten, I. Marcikic, V. Scarani, W. Tittel, H. Zbinden, and N. Gisin, "Tailoring photonic entanglement in high-dimensional Hilbert spaces," Phys. Rev. A **69**, 050304 (2004).
28. Q. Zhang, C. Langrock, H. Takesue, X. Xie, M. Fejer, and Y. Yamamoto, "Generation of 10-GHz clock sequential time-bin entanglement," Opt. Express **16**, 3293–3298 (2008).
29. H. Takesue and B. Miquel, "Entanglement swapping using telecom-band photons generated in fibers," Opt. Express **17**, 10748–10756 (2009).
30. H. Takesue and K. Inoue, "Generation of polarization-entangled photon pairs and violation of Bell's inequality using spontaneous four-wave mixing in a fiber loop," Phys. Rev. A **70**, 031802 (2004).
31. X. Li, P. L. Voss, J. E. Sharping, and P. Kumar, "Optical-fiber source of polarization-entangled photons in the 1550 nm telecom band," Phys. Rev. Lett. **94**, 053601 (2005).
32. H. Takesue and K. Inoue, "1.5-μm band quantum-correlated photon pair generation in dispersion-shifted fiber: suppression of noise photons by cooling fiber," Opt. Express **13**, 7832–7839 (2005).
33. A. Peres, "Separability criterion for density matrices," Phys. Rev. Lett. **77**, 1413–1415 (1996).
34. R. J. Feuerstein, "Field measurements of deployed fiber," in *Optical Fiber Communication Conference and Exposition and the National Fiber Optic Engineers Conference* (OSA, 2005), paper NThC4.